https://doi.org/10.5194/egusphere-2026-1506
Preprint. Discussion started: 26 March 2026

An Assessment of Lunar Photometry in AERONET

Joel Schafer[1,2], Tom F. Eck[2,3], Ilya Slutsker[1,2], Pawan Gupta[2], Mikhail Sorokin[1,2], Alexander Sinyuk[1,2], and Alexander Smirnov[1,2]

[1]Science Systems and Applications, Inc. (SSAI), Lanham, MD 20706, USA
[2]NASA Goddard Space Flight Center (GSFC), Greenbelt, MD 20771, USA
[3]University of Maryland Baltimore County (UMBC), GESTAR II, Baltimore, MD 21250, USA

Correspondence: Joel Schafer (joel.schafer@nasa.gov)

Abstract. AERONET has been acquiring direct beam lunar observations at six wavelengths from 440 to 1640 nm from most newer model T CIMEL sun-sky radiometers in the network for many years and producing a night-time AOD data set, which currently includes observations at 492 sites dating back as far as 2014. The new dataset of lunar AOD now uses an updated empirical correction for the ROLO lunar irradiance model and has been extensively analyzed for all long-term lunar-capable sites by evaluating the continuity of AOD between solar and lunar measurements during limited temporal windows. Comparison of daytime and nighttime AOD measurements shows good agreement at all sites with more than a decade of data with mean differences typically within ± 0.01 for $\mathrm{AOD}_{440\,\mathrm{nm}}$ and similar or better agreement at longer wavelengths. Comparisons during 3-hour transition periods between day and night observations during conditions of low and stable AOD found statistically negligible differences of AOD at all common wavelengths as well as for Ångström Exponent, column water vapor and $\mathrm{AOD}_{\mathrm{fine}}$ and $\mathrm{AOD}_{\mathrm{coarse}}$ parameters from SDA. The lunar AOD product demonstrates consistency with solar AOD across diverse aerosol conditions at AERONET sites globally, validating the empirical correction approach.

1 Introduction

The lunar AOD product from AERONET represents the most globally extensive ground-based database of nighttime AOD available with records at hundreds of sites for more than a decade. When lunar geometry is favorable, nearly full temporal coverage of nighttme AOD can be acquired in contrast to that from satellite sensors often limited to overpass periods. Nighttime AOD can differ significantly from daytime AOD due to potentially higher concentrations (shallower boundary layer), increased relative humidity that enhances hygrostatic growth, differences in emission rates in day versus night, diurnal differences in cloud-aerosol interactions and different chemical evolution pathways in the absence of sunlight [Jiang et al. (2024); Li et al. (2025b); Song et al. (2024)]. These measurements enable research that can provide a more complete picture of the 24-hour aerosol cycle with applications for air quality trends and radiative forcing where at night aerosols commonly have a warming effect in contrast to daytime cooling [Ji et al. (2025)]. Nocturnal radiative forcing can cause radiative fog in moist surface layers which promotes aerosol processing, while monitoring of Arctic haze necessarily relies on lunar measurements as the only option during polar night which can last almost 4 months at high latitude AERONET sites such as Ny-Ålesund (78.92° N) in Svalbard [Wainwright et al. (2021)]. Nighttime observations present unique challenges such as reliance on an irradiance

https://doi.org/10.5194/egusphere-2026-1506
Preprint. Discussion started: 26 March 2026

source (the Moon) that is more variable and much lower in signal than for solar (daytime) observations and current irradiance models are imperfect [Zhu J. et al. (2026)]. A technique relying on the comparison of solar and lunar Langley-derived V_0 (extraterrestrial voltage) was developed to correct for errors in top-of-atmosphere (TOA) lunar irradiance associated with lunar phase angle and generate accurate lunar AOD measurements. Perrone et al. (2022) used 3 years of *provisional* lunar AOD data from a CIMEL sunphotometer at Lecce University to evaluate day-night AOD differences. They compared the average of the last hour of daytime data with the first hour of nocturnal data (and the last hour of nocturnal data with the first hour of solar data), finding that the differences were within the accuracy of the solar AODs. These researchers also found no statistically significant differences in monthly averages of lunar and solar AOD when restricted to common days. Li et al. (2025a) also found that nighttime optical properties, including AOD and AE, are generally consistent with daytime observations in six regions of East Asia, but noted that in polluted areas with high local emissions nighttime AOD and extinction profiles are generally lower than their daytime counterparts, whereas in areas with lower local emissions, nighttime AOD and extinction profiles tend to be equivalent to those during the daytime. This paper assesses the quality of the new lunar AOD product by evaluating the agreement of day and night measurements acquired with the same CIMEL sunphotometer under stable AOD conditions for the full AERONET dataset.

2 Method

AERONET reference CIMELs are calibrated at high altitude observatories at Mauna Loa, Hawaii and Izaña, Canary Islands via the Langley method and the derived V_0 (scaled appropriately for changes in earth-sun distance) can be used reliably to compute solar-based AOD so long as the instrument remains stable [Toledano et al. (2018)]. For solar measured AOD the small uncertainty in these Vo's results in high accuracy AOD for reference instruments ranging from 0.009/m at 340 nm to ~0.002/m in the near infrared, where m is the optical airmass [Eck (1999)]. These V_0 represent the extrapolated instrument response at each wavelength at zero air mass and provide the signal in analog-to-digital units (ADU) or "counts" that would be expected for the top-of-atmosphere (TOA) irradiance, $E_0, solar$. For lunar AOD, the situation is more complicated because lunar irradiance is highly variable with lunar phase angle and the V_0 acquired from any lunar Langley is only valid for the current earth-moon configuration. The ROLO (RObotic Lunar Observatory) model [Kieffer and Stone (2005); Stone et al. (2020)] is the primary means to model lunar spectral irradiance, however it is not well suited as an absolute reference due in part to errors associated with atmospheric effects as it was developed from ground-based measurements. Consequently, early lunar AOD calculations that relied solely on this model for TOA lunar irradiance were not of adequate quality and often produced unphysical results, e.g. large negative AODs during low AOD intervals, see example from AERONET site Goddard Space Flight Center (GSFC) (Figure 1).

Fundamentally this problem can be addressed either by a) correcting the AOD product derived from imperfect irradiance input or b) correcting the irradiance model. Prior work has been done attempting to quantify the systematic dependencies on lunar phase angle and correct for irradiance errors in ROLO based on comparison with star photometry for example [Barreto

https://doi.org/10.5194/egusphere-2026-1506
Preprint. Discussion started: 26 March 2026

et al. (2017); Román et al. (2020)]. Additionally, an alternative lunar irradiance model,the Lunar Irradiance Model of the European Space Agency (LIME) is under development [Toledano et al. (2024)].

Figure 1. AOD at GSFC on Jan 21, 2024 derived with uncorrected and with bias-corrected ROLO TOA irradiance

The strategy developed by AERONET was to correct for the limitations of ROLO irradiance by comparing V_0's from high elevation lunar Langleys with solar Langleys at Mauna Loa Observatory (MLO) and Izaña calibration facilities. For a given instrument, the solar to lunar V_0 ratios should ideally match the sun/sky gain ratio of 4096 [Li et al. (2016)]. Thus, observed deviations from this nominal value could be determined as a function of lunar phase angle (LPA) and used as an empirical correction factor by which the baseline ROLO irradiances are modified. While neither solar nor lunar Langley V_0's are strictly constant due to changing TOA irradiance over time, the solar irradiance changes in a highly predictable manner due to earth-sun distance. By contrast, the variation in lunar irradiance is more rapid and far more complex in nature. It is this variation in lunar irradiance that is particularly challenging to model precisely and this necessitates an empirical correction to the ROLO predicted values in order to compute accurate lunar AOD. Consequently, the process that has been employed is to take the solar V_0, normalized to 1AU, convolved with the TSIS-1 Hybrid Solar Reference Spectrum, V2 [Coddington et al. (2023)] in order to define a spectral irradiance calibration (W/m^2/μm / ADU) for a given instrument. This instrument-specific calibration is then applied, with default sun/sky gain adjustment, to each evaluated $V_{0,lunar}$ to compute the inferred TOA lunar spectral irradiance $E_{0,lunar}$. Finally, this $E_{0,lunar}$ is compared with the modeled $E_{0,ROLO}$ from ROLO for the specific lunar conditions;

https://doi.org/10.5194/egusphere-2026-1506
Preprint. Discussion started: 26 March 2026

lunar phase angle, spectral and angular dependence of reflectance etc. to provide an empirical bias for the full range of moon scenarios. The large set of solar/lunar langley pairs (N > 600 at each wavelength from 440nm to 1640nm) from MLO and Izaña were used to fit a nonparametric local regression (LOESS) model and generate a ***lookup table*** (LUT: 0.8° resolution) of ROLO correction factors for each wavelength as a function of Lunar Phase Angle (LPA). The LPA is defined to be 0° at full moon and 90° (-90°) at waning (waxing) quarter moon. The percentage adjustments for each solar/lunar langley pair necessary for equal day/night V_0's and the associated ROLO LOESS correction fit are shown for the 440nm and 675nm channels in Figure 2. Application of these LUT corrections are found to produce good continuity of AOD across day/night transitions (Figure 3).

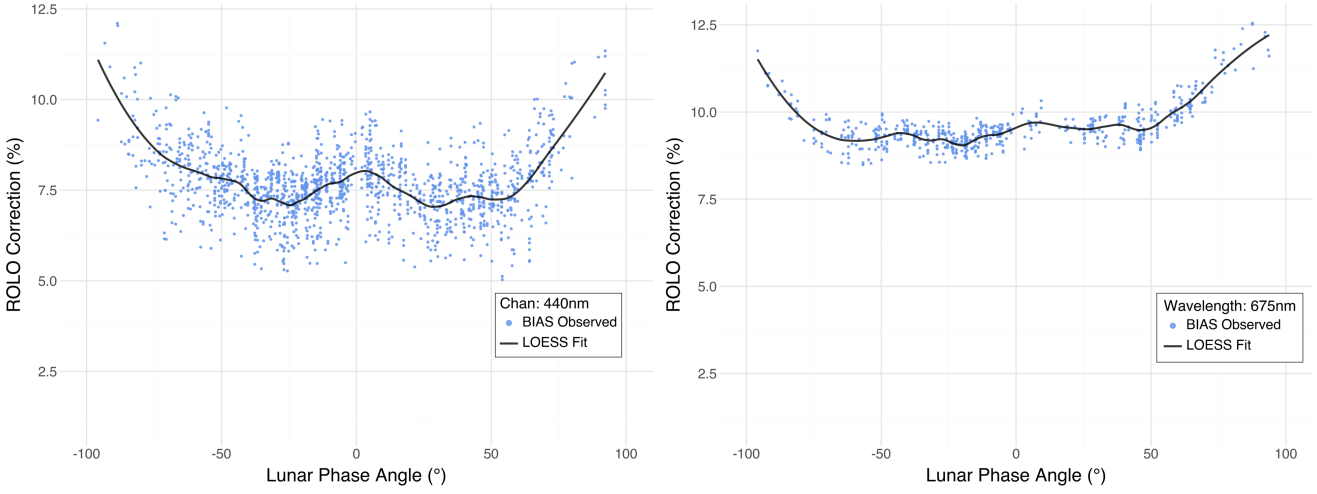

Figure 2. Observed bias in solar/lunar Langley ratios and computed fit for correction (increase) of ROLO irradiance at 440 nm and 675 nm CIMEL wavelengths.

https://doi.org/10.5194/egusphere-2026-1506
Preprint. Discussion started: 26 March 2026

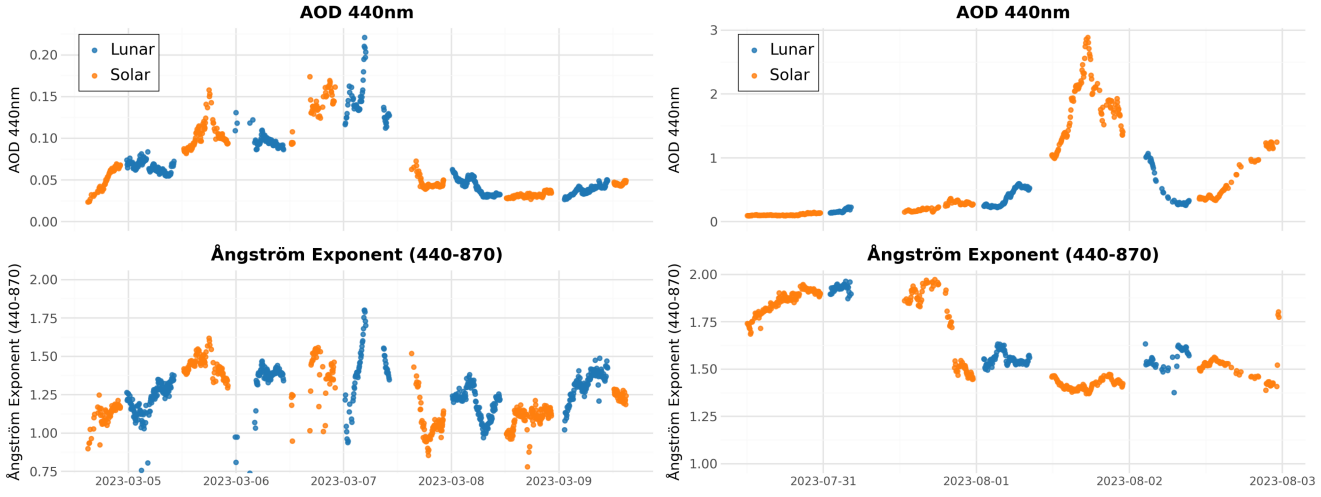

Figure 3. $AOD_{440\ nm}$ and Ångström exponent across day/night transitions for a low and high AOD interval at Goddard Space Flight Center

3 Unique Aspects of Lunar Versus Solar AOD

3.1 Moon as Irradiance Source

Solar AOD calculations rely on the sun as a very stable source at top-of-atmosphere (TOA) with earth-sun distance on an annual cycle as the primary cause of changes in expected irradiance. While the sun is ultimately the source of the moon's reflected light, the lunar irradiance for an Earth observer additionally varies as function of lunar phase angle (LPA), i.e., the fractional illumination as viewed from the surface) on a monthly scale with changes of significance to AOD over much smaller time intervals. The lunar surface itself is comprised of material types correlated with a range of albedos that affect lunar brightness depending on the particular portion of the moon that is illuminated, and the reflected light is further influenced by surface features that also vary with viewing angle. Although solar irradiance varies by $\pm 3.4\%$ over the course of a year (with an additional small fluctuation due to an 11-year cycle of solar activity of 0.1%), this is a simple geometric effect that can be corrected accurately and precisely. By contrast, the lunar irradiance can change by a percentage comparable to the annual solar change in 5-6 hours or only 2-3 hours in the period near a full moon. For the full moon period, this is due to a number of causes including the oppositional effect ('heiligenschein') where the highly porous lunar regolith structure produces multiple scatter of the returned light that constructively interferes [Hapke et al. (1998)]. This phenomenon is further complicated by the occurance of 'shadow-hiding', a purely mechanical effect where the normally incident sunlight causes any shadows cast by lunar material to be hidden by the material itself resulting in substantial ($\sim$40%) increases in lunar brightness in the full moon intervals (LPA: -5° to +5°) which only lasts $\sim$ 20 hours. The lunar brightness at full moon is 10x or more that at quarter moon representing an extremely large span of values over the range of lunar phase angles in which CIMEL measurements are made. Even outside of the full moon window, the change in signal from near full moon to quarter moon might be a 7:1 ratio which is much larger

https://doi.org/10.5194/egusphere-2026-1506
Preprint. Discussion started: 26 March 2026

than expected if one simply assumed a sphere with lambertian scattering (∼3:1), again a consequence of backscatter effects of irregular lunar regolith surface features. Additionally, the variation of earth-moon distance produces a variation of irradiance of ±12% within two weeks from apogee to perigee. While the effects on lunar irradiance related to orbital geometry such as the non-linear phase function can be definitively modeled, computing the lunar signal remains far more challenging than that for the solar signal due the inhomogeneous and structurally complex lunar surface as well as spectral differences in reflectance and much smaller time scales of variation. Lower signal from the lunar source also precludes estimation of AOD for the UV channels and leads to increased triplet variability (variation of AOD taken at three discrete measurement times within a one minute interval), particularly when both lunar phase angle (LPA) and lunar zenith angle (LZA) are large.

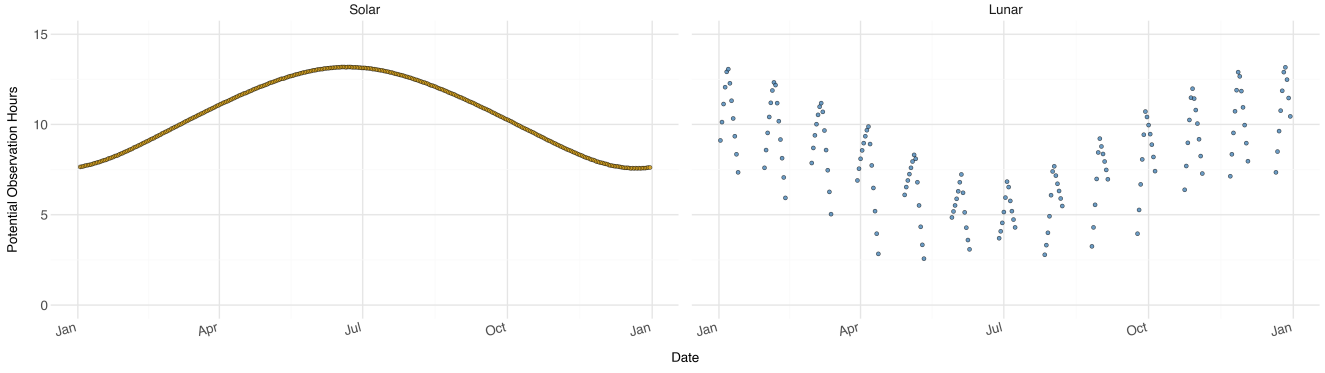

Figure 4. Comparison of solar and lunar potentially measureable hours at GSFC (38.99° N,-76.84° W) for one year

3.1.1 Difference in observational periods of solar and lunar AOD

While the daylength varies gradually over the course of the year, the corresponding night interval of lunar AOD cycles much more rapidly and can differ greatly in duration from that available for sun measurements; see example for one year at GSFC. Figure 4 presents the maximum day duration of solar AOD collection (SZ <= 82°) and the observable lunar interval refers to data when LPA is within the range -90° and 90° and when the solar zenith angle >= 98° (to avoid solar contamination). The solar day at GSFC varies by about 5.5 hours throughout the year, whereas observable lunar night duration can change by more than this (∼ 7 hours) in less as few as 6 days and the annual trend is the inverse of the solar trend. Consequently, the difference between solar and lunar measurement windows can be significant at times. Additionally, the lunar phase angle constraints also limit the lunar AOD window to approximately half of every month period (typically allowing for 12-14 days of possible measurements) thus, solar and lunar AOD datasets differ markedly in temporal coverage on both daily and monthly time scales.

https://doi.org/10.5194/egusphere-2026-1506
Preprint. Discussion started: 26 March 2026

4 Evaluation of Lunar AOD

4.1 Assessing Bias Correction

The applied adjustment to lunar irradiance due to the empirical bias correction can often be a large factor ($\sim 10\%$) so it's critically important to examine the resulting product for potential bias. For this purpose, the most straightforward standard of comparison would be the associated solar AOD for the same instrument. While the sun and moon measurement periods are mutually exclusive, the transition interval from day to night and vice versa provides an opportunity to quantify differences in this relatively short window for hundreds of sites on a large number of suitable days. Due to the need to avoid solar contamination of the signal, lunar AOD could not be acquired unless the sun was significantly below the horizon (SZA > 98°) which results in at least a couple hours without data following the final solar AOD measurement even if the moon is above the horizon at sunset (likewise lunar measurements will be precluded for some duration prior to sunrise). This transition interval was standardized for all sites by computing the mean and standard deviation of the average AOD difference for all 3-hour windows during the period which included an hour of both day and night measurements with at least 6 observations in each day/night average (measurement protocol nominally has observation every 5 minutes). Since the nighttime *calibration accuracy* was specifically being examined in this exercise, the hour averaged data were also restricted to cases of low AOD with small standard deviation ($\mathrm{AOD}_{440\ \mathrm{nm}} \leq 0.1$ and std < 0.01) for both solar and lunar intervals to minimize the effects of potential cloud influence– though the choice of thresholds had little effect on the results. Figure 5 and Figure 6 show these transition AOD 440_{nm} differences from data aquired at 372 sites measured with 454 different CIMELs vs lunar phase angle (LPA) and lunar zenith angle (LZA). The degree of agreement between solar and lunar AOD is not notably dependent on LZA despite lower signal at large lunar zenith while there is some varying structure to the differences in Figure 5 as a function of LPA suggesting the complexities of lunar irradiance are not always perfectly bias-corrected though the deviations are minor, and diminish with increasing wavelength. In addition to comparing solar/lunar AOD differences across this transition, a similar comparison of the average and standard deviation of AOD difference was made with a similar time window gap entirely within the solar day and lunar night as a point of reference for typical agreement of AOD for such a 3-hour time lag.

https://doi.org/10.5194/egusphere-2026-1506
Preprint. Discussion started: 26 March 2026

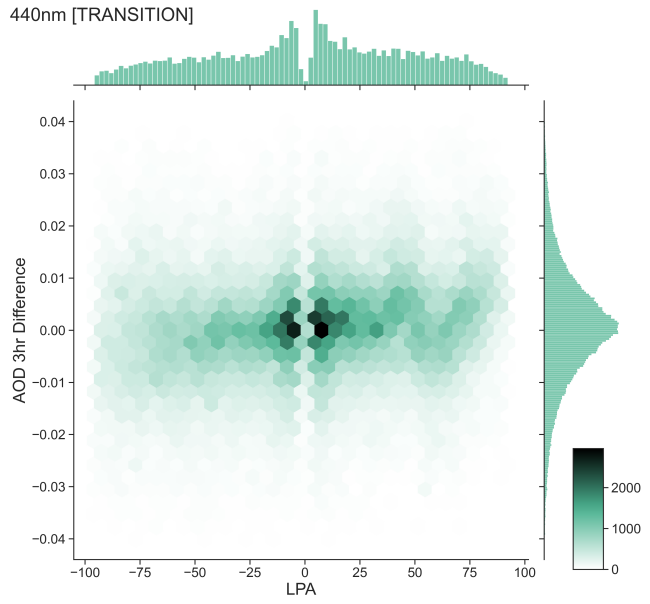

Figure 5. Difference in 3 hour window $AOD_{440\ nm}$ for transition from day to night (night to day) vs lunar phase angle from 372 sites (N=281,159)

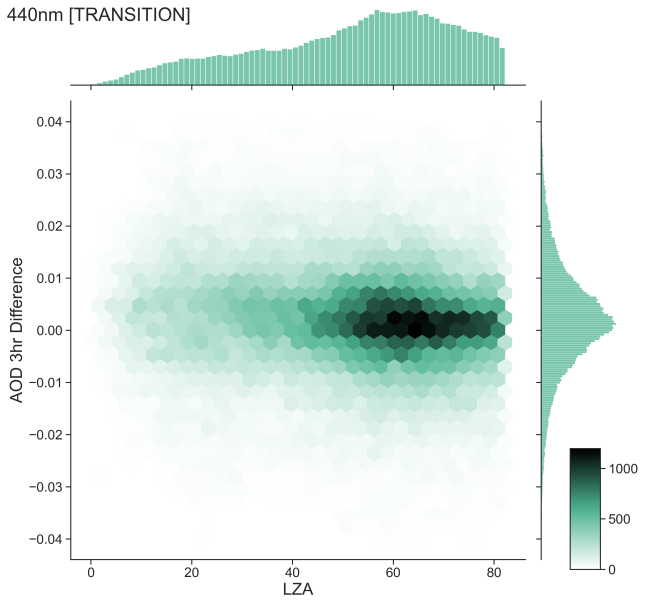

Figure 6. AOD difference as in Figure 5 shown vs lunar zenith angle

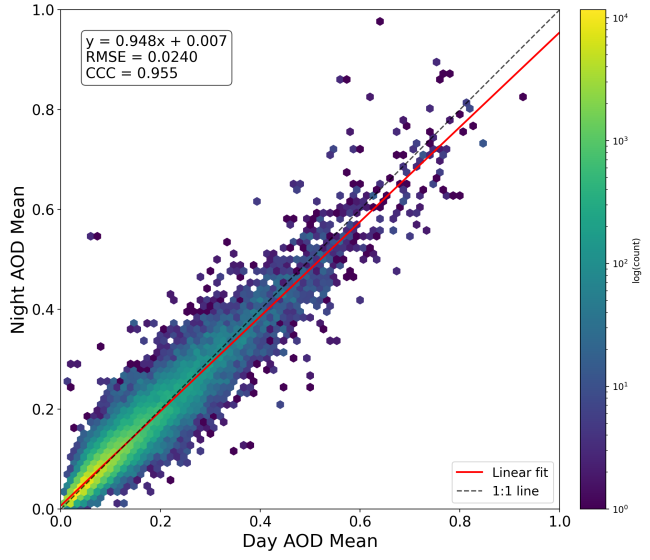

Figure 7. Difference in 3 hour window $AOD_{440\ nm}$ difference for transition from day to night ($AOD_{440\ nm}$ <= 1.0, N=212,000)

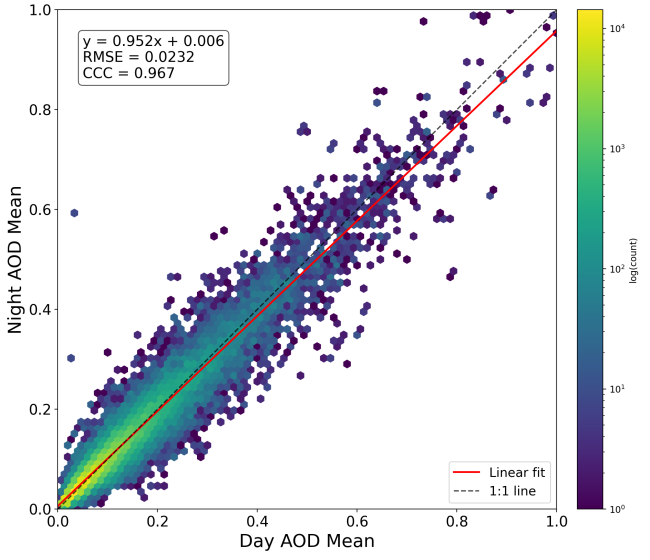

Figure 8. Difference in 3 hour window $AOD_{440\ nm}$ for transition from night to day ($AOD_{440\ nm}$ <= 1.0, N=252,273)

https://doi.org/10.5194/egusphere-2026-1506
Preprint. Discussion started: 26 March 2026

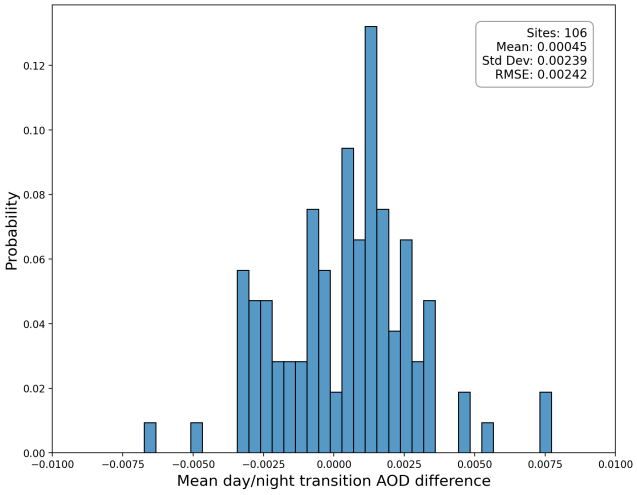

Figure 9. Histogram of mean $AOD_{440\ nm}$ differences for all sites with more than 500 transition comparison events (N=106 sites)

Additional statistical analysis was restricted to 24-hour periods containing all three measurement types: daytime solar AOD, nighttime lunar AOD, and transition AOD differences in order to maximize the commonality of the comparison. For every wavelength, the mean AOD differences across the transition from day-night (night-day) are negligibly small and similar or smaller than the differences observed within day or within night periods implying the absence of systematic bias in the lunar AOD (Table 1) as well as Ångström exponent (440-870nm), Precipitable Water Vapor, fine and coarse mode AOD from the Spectral Deconvolution Algorithm (SDA) of O'Neill et al. (2003). (Table 2). While the statistics in these tables are for low AOD conditions, Figures 7 and 8 show the night to day and day to night to day AOD correspondence up to $AOD_{440nm} = 1.0$ which adds data from an additional 50 sites previously excluding by the 0.1 AOD limit. Good agreement of the solar and lunar AOD is also observed for individual sites as depicted in Figure 9. This histogram shows all AERONET sites with more than 500 transition comparision events acquired from at least 50 different days (N=106 sites) and demonstrates that all these locations had average $AOD_{440\ nm}$ differences between day and night less than ± 0.01.

Table 1. 3-hour Time Interval AOD Difference Statistics by Interval
(Means are computed from the set of interval averages from common 24-hour windows)

	440nm		500nm		675nm		870nm		1020nm		1640nm	
Interval Type	Mean	StDev	Mean	StDev	Mean	StDev	Mean	StDev	Mean	StDev	Mean	StDev
Transition	0.0003	0.0112	0.0005	0.0096	0.0001	0.0077	0.0002	0.0069	0.0004	0.0075	0.0003	0.0059
Day Only	-0.0015	0.0077	-0.0012	0.0067	-0.0007	0.0051	-0.0009	0.0047	-0.0006	0.0044	-0.0008	0.0041
Night Only	0.0011	0.0085	0.0008	0.0074	0.0006	0.0059	0.0005	0.0054	0.0003	0.0055	0.0005	0.0048

https://doi.org/10.5194/egusphere-2026-1506
Preprint. Discussion started: 26 March 2026

Table 2. 3-hour difference of Ångström Exponent, precipitable water (cm), SDA AOD fine and coarse mode components for transition

AE		WV		AOD_Fine		AOD_Coarse	
Mean	StDev	Mean	StDev	Mean	StDev	Mean	StDev
0.0018	0.0960	0.0377	0.1746	-0.0026	0.0221	0.0011	0.0165

4.2 Potential effects of differences in cloud-screening for lunar data

The cloud-screening protocols for lunar AOD are the same as for solar AOD with one exception. The lunar measurement sequence does not perform the cross-scan scenario (sky radiance measurements across the aureole during solar operation) which is used to identify clouds via the 'curvature' check in the cloud-screening algorithm (Giles et al. (2019)). This is primarily a check for thin cirrus clouds that are relatively uniform in space and time therefore not easily detected by the temporal variance checks in AERONET cloud screening. It's not possible to *definitively* determine the effect of omitting this check however we have attempted to estimate this by looking at the solar AOD data with only the curvature test disabled (other checks applied normally) and comparing the results to the standard cloud-screened data. The data removed by the curvature check represents only a subset of the total cloud-screened data in that the majority of cloud-influenced observations will have already been removed by triplet variability and daily time series variability checks in the preceding QC processing. Further, there is a practical limit to the range where curvature can reliably distinguish thin cirrus clouds from aerosols with effectiveness dropping off as the AOD becomes large, thus isolating the consquences of lacking curvature check is a nuanced assessment.

Both monthly and daily averages of AOD and Ångström exponent (AE) were computed for the solar AOD record at 259 sites

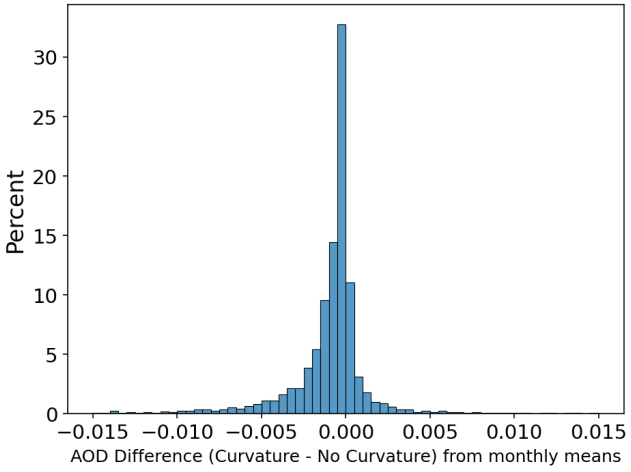

Figure 10. Difference in $AOD_{440\,nm}$ multi-year month averages with and without curvature check

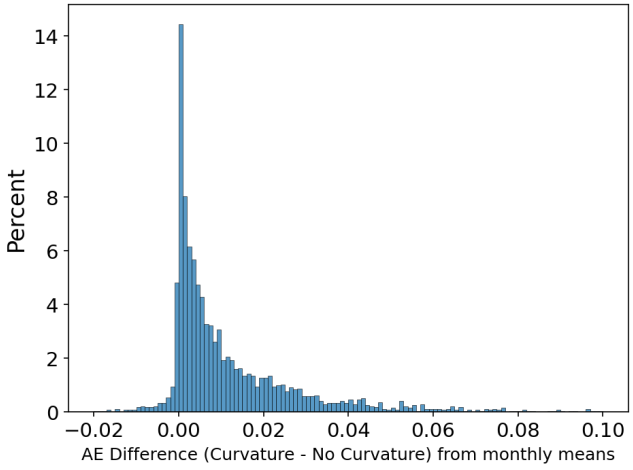

Figure 11. Difference in AE multi-year month averages with and without curvature check

with and without curvature check included in the cloud-screening. While there is an expected tendency of reduced AOD and

https://doi.org/10.5194/egusphere-2026-1506
Preprint. Discussion started: 26 March 2026

increased AE when curvature check is utilized, the typical monthly differences are negligible (Figure 10 and Figure 11). Aggregated multi-year monthly average differences by site (curvature-no_curvature) of AOD 440_{nm} are very small ranging from -0.0004 to -0.0014 and 97% of the individual monthly means had mean AOD differences of < 0.01 while 7% of months had no difference. The differences shown in Figure 10 and Figure 11 are multi-year month averages so individual months would be expected to exceed this.

However, even when monthly AOD and AE are considered individually, the statistical differences are typically quite small. Of 14,810 individual months, only 9 months (0.1%) had a mean AOD difference greater than 0.02 and only 41 (0.3%) had a mean AE difference greater than 0.1 when removing the curvature check. The potential for significant changes in daily averages is larger but even so only 1.1% of days had an increase of $\mathrm{AOD}_{440\,\mathrm{nm}} > 0.02$ and 2% had an increase in AE > 0.1 ($\mathrm{mean\_AOD\_diff}_{440\,\mathrm{nm}} = 0.002$, $\mathrm{mean\_AE\_diff} = 0.0002$). Therefore, in general the lack of curvature check would not normally be expected to have notable consequences for the lunar AOD cloud-screening, but note that there are seasonal intervals where changes in Ångström exponent is more pronounced and may be significant in some regions, such as southeast Asia often in association with monsoonal activity and a small number of locations had 5-10% of the data record where day average AE was > 0.1 lower without the curvature check. Even when the absence of curvature check doesn't profoundly affect mean AOD or AE, the additional number of observations removed can be substantial. For instance, at the AERONET site in Singapore the use of curvature removes 8,351 more data points during the 2016-2024 interval than are removed without this screening mechanism, a 5.1% higher exclusion rate.

It should be noted that additional cloud-screening checks are being developed which are only applicable to daytime measurements so it's possible that disparity in cloud-screening efficiency will be greater in future versions of the database. Conversely, additional future cloud screening of AOD and AE time series by AI/ML algorithms may potentially result in a reduction in differences between solar versus lunar cloud screening.

5 Low Signal and Measurement Limitations

Aerosol optical depth (AOD) measurements require sufficient direct-beam irradiance to ensure that diffuse light contributions to the direct beam don't result in an apparent AOD that is lower than the true value [Sinyuk et al. (2012); Kinne et al. (1997)]. To ensure this condition, AERONET applies a minimum signal threshold for valid sunphotometer measurements, defined as $V_{\mathrm{min}} = V_0/1500$ where V_0 is the instrumental top-of-atmosphere signal. This minimum required signal imposes an inherent operational upper limit to the AOD that can be measured by solar or lunar photometry. Note that the V_0 values are significantly smaller for lunar measurements as compared to solar measurements and the variation of V_0 for lunar measurements is much greater as a function of lunar phase.

For both solar and lunar AOD, there is the potential for low signal observations to be excluded, an event which occurs with higher frequency as aerosol optical depth increases and disproportionately affects shorter wavelengths that typically have higher AOD, particularly when Ångström exponent is moderate or large. An effect of the lower reflected irradiance of the moon is that the lunar measurements experience even more significant reductions than solar observations. Although these

https://doi.org/10.5194/egusphere-2026-1506
Preprint. Discussion started: 26 March 2026

considerations don't impact the accuracy of retained lunar AOD data, these factors may complicate comparisons of statistics between solar and lunar intervals especially when AOD is large enough that the reduced maximum AOD of lunar observations becomes relevant.

5.1 Empirical Maximum AOD

To quantify this measurement limitation, the solar AOD dataset for all sites with significant lunar AOD record were combined and the maximum possible AOD was empirically estimated by finding the largest recorded AOD in airmass bins and an exponential equation was fit (Figure 12). The same process was repeated using the lunar data record, but the lunar data were further divided into 3 lunar phase angle groups since maximal signal is substantially affected by this phase.

Assuming the AERONET operational threshold $V_{\min}$, the maximum solar total atmospheric optical depth (Rayleigh plus aerosol plus gaseous) follows from the Beer-Lambert law where m is the optical airmass:

$$\tau_{\max}(m) = \frac{1}{m} \ln\left(\frac{V_0}{V_{\min}}\right) \implies \tau_{\max}(m) = \frac{1}{m} \ln(1500)$$

This limit allows for accurate total OD values up to 7.31 at an airmass of 1 [Giles et al. (2019)]. and 1.05 at an airmass of 7 which is consistent with observed 440 nm maxima of 6.91 and 0.99 in this AERONET solar AOD dataset. Note that the Rayleigh optical depth at 440 nm is 0.243 for mean sea level pressure [Bodhaine et al. (1999)] and gaseous absorption OD is typically <0.01 at this wavelength. The maximum AOD limit has also been observed from solar measurements in very high smoke AOD cases in Indonesia in 2015 with a maximum AOD at 675 nm of 7.1 [Eck et al. (2019)].

The complexities of lunar geometric dynamics make theoretical calculations of lunar maximum AOD more challenging so empirical determination of these potential limits is a useful estimation. Consistent with expectations, the periods with 'bright moon' conditions (small LPA; < 22.5°; and illumination of lunar disk > 96%) have the largest observed AOD at all airmass ranges as would be expected. The lunar intervals that represent the minimum illumination allowed for lunar observations (large LPA; > 72.5°; 50-65% illumination) have a maximum observable AOD that is approximately half that of the bright moon conditions and 3x less than the corresponding solar AOD maximum.

https://doi.org/10.5194/egusphere-2026-1506
Preprint. Discussion started: 26 March 2026

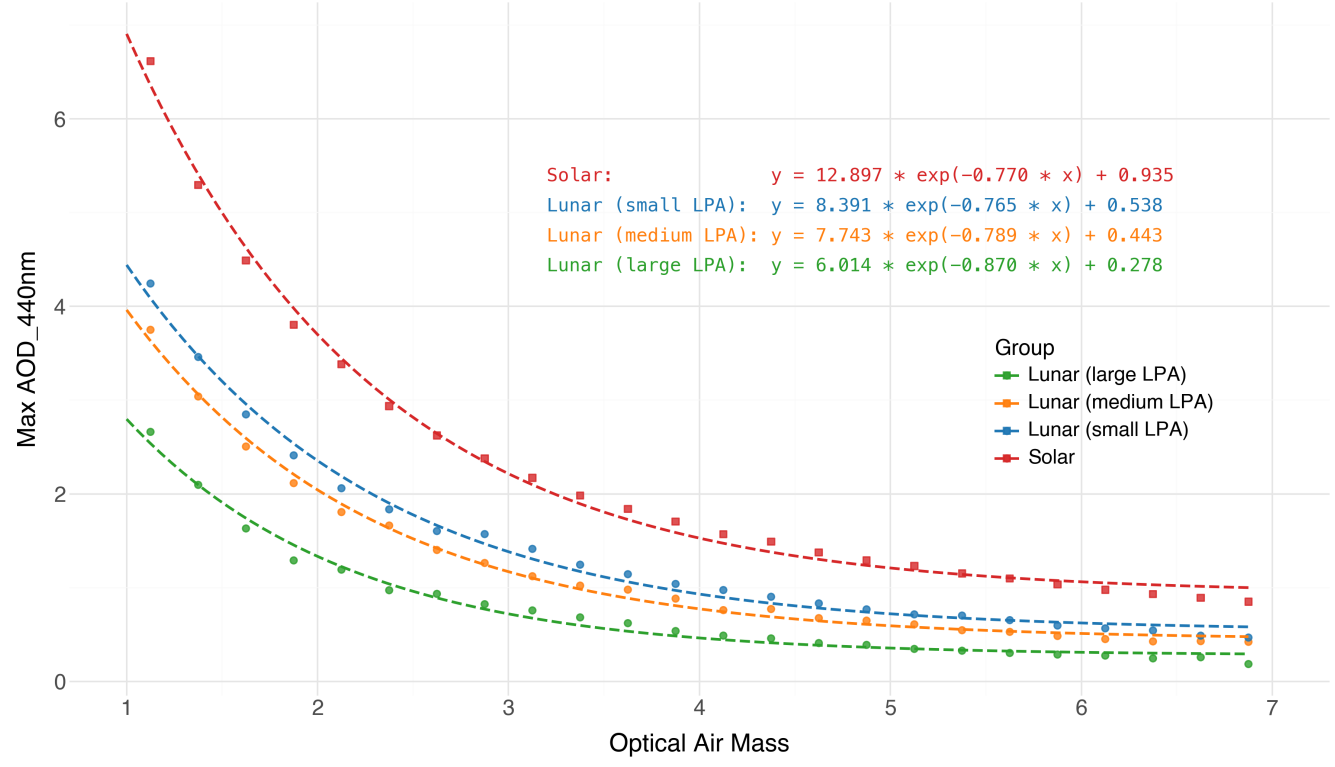

Figure 12. Maximum observed $AOD_{440\,nm}$ in airmass bin for solar and lunar (three lunar phase angle ranges) dataset

5.2 High AOD Exclusion and Statistical Effects

Figure 13 shows lunar and solar AOD data from Ilorin, Nigeria an AERONET site that experiences significant Saharan dust as well as seasonal biomass burning aerosol. In this figure, the AOD observations have been partitioned by AOD bin and airmass range. The relative contribution of AOD in each AOD bin is shown and as air mass increases the fraction of higher AOD decreases as available signal decreases (larger zenith angles). While this is observed for each measurement type (solar/lunar), the elimination of the higher AOD components at large airmass is much more pronounced for lunar data. Note that the proportional contribution from each AOD bin range is similar for lunar (top) and solar (bottom) for small airmass (AM <= 2). Both solar and lunar measurements see attrition at larger airmass (AM >= 4) due to inadequate signal but the lunar fractional contribution from lower AOD increases more substantially and observations from the three bins of largest AOD are entirely excluded while solar observations lose only the two largest AOD bins. The broader consequence of this signal limitation on the AERONET data record is *sampling bias*, specifically truncation of large AOD observations as AOD (and airmass) increases, primarily for shorter wavelengths. This aspect is directly reflected in Figures 14a and 14b which are $AOD_{440\,nm}$ histograms composited for common day data from 201 sites based on all 24-hour periods with five or more L2 observations from both day and night (> 5 million measurements of both lunar and solar data). These lognormal plots [O'Neill et al. (2000)] show the increasing loss

https://doi.org/10.5194/egusphere-2026-1506
Preprint. Discussion started: 26 March 2026

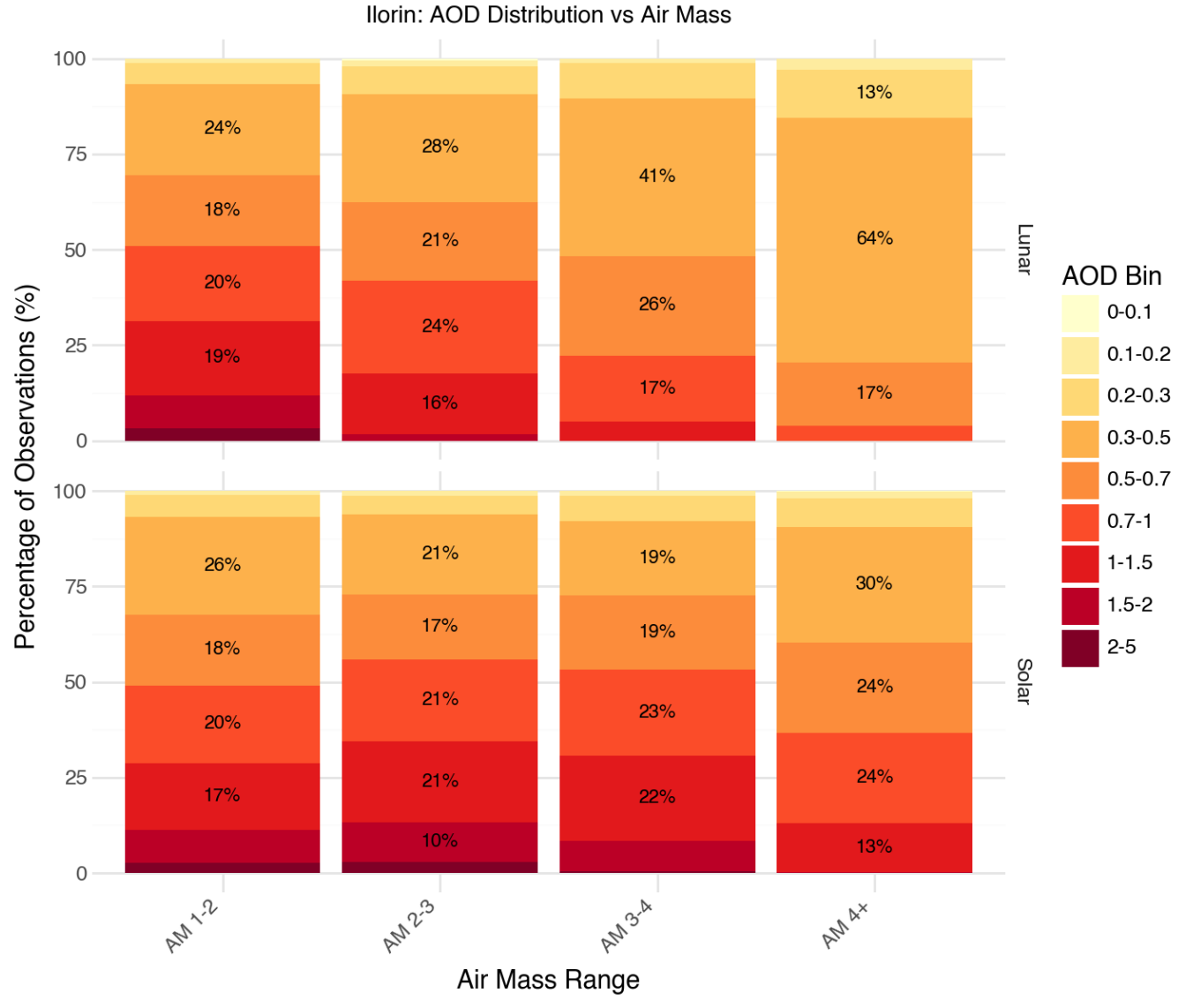

Figure 13. $AOD_{440\,nm}$ distribution vs Airmass for solar and lunar data restricted to common days (Ilorin, Nigeria)

https://doi.org/10.5194/egusphere-2026-1506
Preprint. Discussion started: 26 March 2026

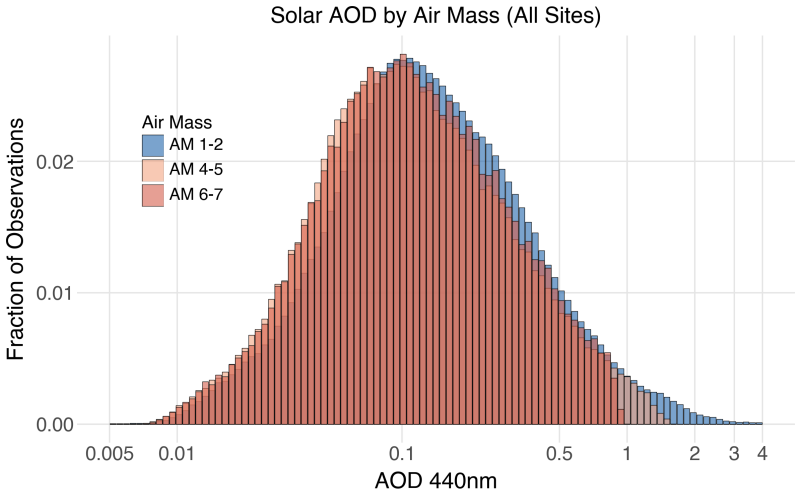

(a) Solar

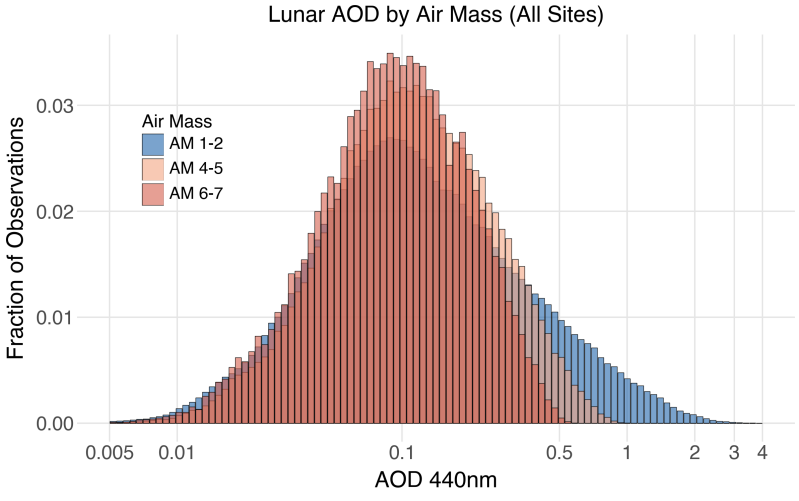

(b) Lunar

Figure 14. Comparison of $AOD_{440\,nm}$ histograms by airmass for 201 AERONET sites. (Data restricted to common day set)

of higher AOD for both solar and lunar observations at larger airmass, with disproportionately larger such effect for the lunar dataset.

For this set of 201 sites, the average lunar removal percentage (from the L2 AOD dataset) for the 440nm channel is 3.2%, while the corresponding rates at 675nm and 870nm are quite small (0.3% or less). However, this doesn't imply that the longer wavelengths don't also experience loss due to low signal rejection as there are cases when no channels reach Level 2 data status. The lunar data display much larger (3x) removal rates for 440nm than do solar data as would be expected due to the lower possible maximum AOD for lunar measurements. Although overall the percentage of AOD that are excluded is small,

https://doi.org/10.5194/egusphere-2026-1506
Preprint. Discussion started: 26 March 2026

the fractional loss of AOD can be significant for higher AOD locations with some sites excluding more than 8% of L2 lunar measurements at 440nm. The general pattern is that more observations are excluded as AOD increases and typically there is greater removal for lunar than solar measurements. The AOD removal rates for solar and lunar observations by wavelength are computed for a selection of individual sites (Table S1, in the Supplement).

Figure 15 presents data from the AERONET site Palangkaraya where high AOD events are frequent. Figure 15a shows histograms of all L2 $AOD_{870\ nm}$ which are overlaid with histograms of the $AOD_{870\ nm}$ measurements from just the subset where $AOD_{440\ nm}$ values have been excluded. Figure 15b shows the percentage of L2 data with an AOD measurement at $AOD_{870\ nm}$ but not at $AOD_{440\ nm}$ for the solar and lunar datasets. As expected, the absence of $AOD_{440\ nm}$ is typically found when $AOD_{870\ nm}$ is large, with an earlier onset of this feature for the lunar data. As AOD increases the fraction of L2 $AOD_{870\ nm}$ measurements with no associated $AOD_{440\ nm}$ becomes substantial and is normally greater for the lunar AOD where the Level 2 data often have 100% of AOD 440nm observations excluded for the highest aerosol loading cases.

https://doi.org/10.5194/egusphere-2026-1506
Preprint. Discussion started: 26 March 2026

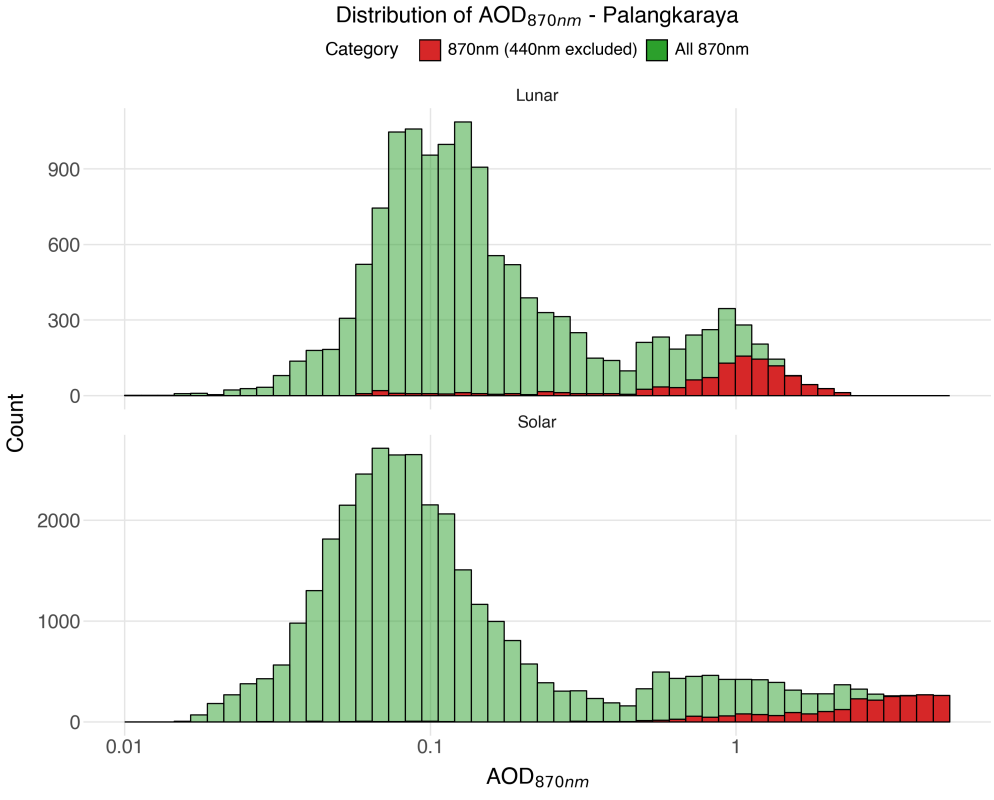

(a) Histogram of $AOD_{870\,nm}$ when $AOD_{440\,nm}$ is absent

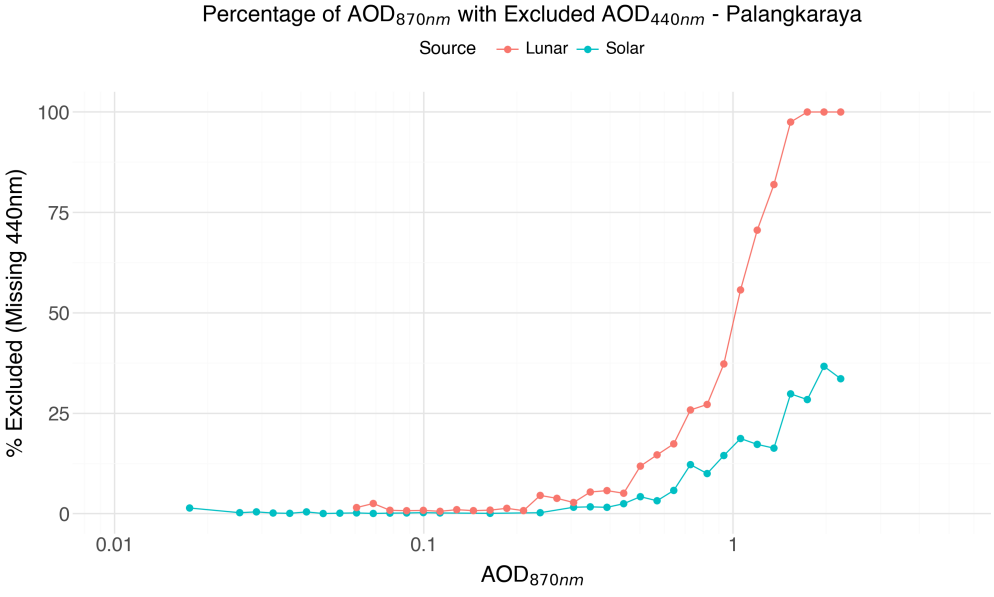

(b) Fraction of Level 2 $AOD_{870\,nm}$ without $AOD_{440\,nm}$

Figure 15. Exclusion of Level 2 Solar and Lunar $AOD_{440\,nm}$

https://doi.org/10.5194/egusphere-2026-1506
Preprint. Discussion started: 26 March 2026

Despite this selective reduction in higher AOD data, the great majority of observations at a given site are for the airmass range from 1-2 when the available signal is maximal and sampling bias is not impactful. Thus when comparing solar and lunar AOD distributions for *all airmass* levels, with sites sorted as either low (<$AOD_{440\,nm}$> <= 0.2) or high (>= 0.4) AOD sites, the statistics of composited distributions of day and night observations are typically similar for both measurement types (LOW AOD: solar= 0.124 $\pm$ 0.137; lunar= 0.118 $\pm$ 0.117 HIGH AOD: solar= 0.658 $\pm$ 0.492; lunar= 0.636 $\pm$ 0.434) (Figure S1 in the Supplement).

5.3 AOD Triplet Variability

AERONET AODs are computed as the mean of a triplet of measurements taken at 30 second intervals over a one-minute period and diminished signal has effects on triplet variability. The triplet variability (max-min) is one metric used to screen for cloud presence and if the triplet variability of any longer wavelength (675nm, 870nm, 1020nm) exceeds a dynamically defined threshold [Giles et al. (2019)] it will typically be screened as cloudy. In most cases such measurements are excluded though there is a provision to 'add back' a subset of these cases if there are additional factors (such as high Ångström Exponent) providing confidence that the variability is due to aerosol only. Differences exist in the variability of the measurements depending on the type (lunar, solar) with larger triplets observed for dimmer lunar phase periods than during near full moon conditions which may result in larger AOD uncertainty under those conditions (Figure 16). In general, triplet variability is larger for lunar observations than solar observations (Figure 17). These figures present variability of $AOD_{440\,nm}$ which has no *explicit* threshold since as noted the filtering for triplet variablity is only applied to longer wavelengths.

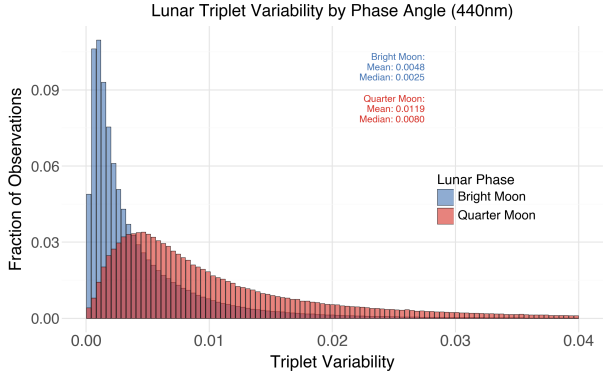

Figure 16. Lunar triplet variability by Phase Angle ($AOD_{440\ nm}$)

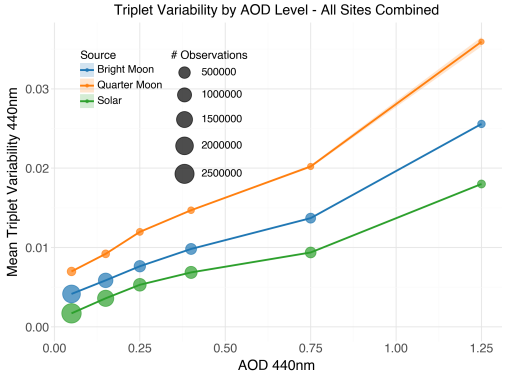

Figure 17. $AOD_{440\ nm}$ triplet variability by AOD and type

6 Conclusions

This study presents a comprehensive assessment of lunar photometry for aerosol optical depth (AOD) retrieval in the AERONET network. The AERONET lunar AOD methodology employs empirical corrections to the ROLO lunar irradiance model based on solar/lunar Langley calibration pairs from high-altitude observatories at Mauna Loa and Izaña.

https://doi.org/10.5194/egusphere-2026-1506
Preprint. Discussion started: 26 March 2026

Lunar measurements face inherent limitations due to lower signal levels compared to solar observations. Very low signal of sky radiances at night preclude angular measurements of the nighttime sky brightness, therefore retrieval of aerosol size distributions and single scattering albedo which are made in daytime by AERONET are not possible at night. There exist differences in cloud screening due to a lack of measurements of sky radiance at night, resulting in slightly more thin cirrus contamination in lunar AOD data as compared to solar AOD. The maximum observable AOD for lunar measurements is approximately 2-3 times lower than for solar measurements which results in greater exclusion rates of shorter wavelength AOD for lunar observations than solar observations when AOD is large.

The temporal coverage of lunar and solar AOD differs substantially due to lunar phase constraints and the inverse relationship between observable solar and lunar periods throughout the year. Lunar observations are limited to approximately 12–14 days per month when lunar phase angle is within the -90 to +90° operational range, providing complementary coverage to daytime measurements but with distinct diurnal and seasonal sampling patterns.

Overall, AERONET lunar photometry provides reliable nighttime AOD measurements that extend aerosol monitoring capabilities beyond daylight hours, enabling improved characterization of aerosol diurnal variability and detection of nighttime aerosol events that would otherwise be unobserved.

Data availability. AOD data for sites used in this study can be acquired at: https://aeronet.gsfc.nasa.gov/new_web/webtool_aod_v3.html

https://doi.org/10.5194/egusphere-2026-1506
Preprint. Discussion started: 26 March 2026

References

Barreto, Á., Román, R., Cuevas, E., Berjón, A. J., Almansa, A. F., Toledano, C., González, R., Hernández, Y., Blarel, L., Goloub, P., Guirado, C., and Yela, M.: Assessment of Nocturnal Aerosol Optical Depth from Lunar Photometry at the Izaña High Mountain Observatory, Atmospheric Measurement Techniques, 10, 3007–3019, https://doi.org/10.5194/amt-10-3007-2017, 2017.

Bodhaine, B. A., Wood, N. B., Dutton, E. G., and Slusser, J. R.: On Rayleigh Optical Depth Calculations, Journal of Atmospheric and Oceanic Technology, 16, 1854–1861, https://doi.org/10.1175/1520-0426(1999)016<1854:ORODC>2.0.CO;2, 1999.

Coddington, O. M., Richard, E. C., Harber, D., Pilewskie, P., Woods, T. N., Snow, M., Chance, K., Liu, X., and Sun, K.: Version 2 of the TSIS-1 Hybrid Solar Reference Spectrum and Extension to the Full Spectrum, Earth and Space Science, 10, e2022EA002 637, https://doi.org/10.1029/2022EA002637, 2023.

Eck, T. F.: Wavelength Dependence of the Optical Depth of Biomass Burning, Urban, and Desert Dust Aerosols, Journal of Geophysical Research: Atmospheres, 104, 31 333–31 349, https://doi.org/10.1029/1999JD900923, 1999.

Eck, T. F., Holben, B. N., Giles, D. M., Slutsker, I., Sinyuk, A., Schafer, J. S., Smirnov, A., Sorokin, M., Reid, J. S., Sayer, A. M., Hsu, N. C., Shi, Y. R., Levy, R. C., Lyapustin, A., Rahman, M. A., Liew, S.-C., Cortijo, S. V. S., Li, T., Kalbermatter, D., Keong, K. L., Yuggotomo, M. E., Aditya, F., Mohamad, M., Mahmud, M., Chong, T. K., Lim, H.-S., Choon, Y. E., Deranadyan, G., Kusumaningtyas, S. D. A., and Aldrian, E.: AERONET Remotely Sensed Measurements and Retrievals of Biomass Burning Aerosol Optical Properties During the 2015 Indonesian Burning Season, AGU Journals, 2019.

Giles, D. M., Sinyuk, A., Sorokin, M. G., Schafer, J. S., Smirnov, A., Slutsker, I., Eck, T. F., Holben, B. N., Lewis, J. R., Campbell, J. R., Welton, E. J., Korkin, S. V., and Lyapustin, A. I.: Advancements in the Aerosol Robotic Network (AERONET) Version 3 Database – Automated near-Real-Time Quality Control Algorithm with Improved Cloud Screening for Sun Photometer Aerosol Optical Depth (AOD) Measurements, Atmospheric Measurement Techniques, 12, 169–209, https://doi.org/10.5194/amt-12-169-2019, 2019.

Hapke, B., Nelson, R., and Smythe, W.: The Opposition Effect of the Moon: Coherent BackscatterandShadow Hiding, Icarus, 133, 89–97, https://doi.org/10.1006/icar.1998.5907, 1998.

Ji, D., Palm, M., Buschmann, M., Ebell, K., Maturilli, M., Sun, X., and Notholt, J.: Hygroscopic Aerosols Amplify Longwave Downward Radiation in the Arctic, Atmospheric Chemistry and Physics, 25, 3889–3904, https://doi.org/10.5194/acp-25-3889-2025, 2025.

Jiang, X., Wang, Y., Tao, M., Wang, J., Zhou, M., Bai, X., and Lu, G.: Characteristics of Daytime-And-Nighttime AOD Differences Over China: A Perspective From CALIOP Satellite Observations and GEOS-Chem Model Simulations, Journal of Geophysical Research: Atmospheres, 129, https://doi.org/10.1029/2023JD039158, 2024.

Kieffer, H. H. and Stone, T. C.: The Spectral Irradiance of the Moon, The Astronomical Journal, 129, 2887–2901, https://doi.org/10.1086/430185, 2005.

Kinne, S., Akerman, T. P., Shiobara, M., Uchiyama, A., Heymsfield, A. J., Miloshevich, L., Wendell, J., Eloranta, E., Purgold, C., and Bergstrom, R. W.: Cirrus Cloud Radiative and Microphysical Properties from Ground Observations and in Situ Measurements during FIRE 1991 and Their Application to Exhibit Problems in Cirrus Solar Radiative Transfer Modeling, Journal of the Atmospheric Sciences, 54, 2320–2344, https://doi.org/10.1175/1520-0469(1997)054<2320:CCRAMP>2.0.CO;2, 1997.

Li, J., Jin, J., Wong, M. S., Wang, J., Lee, K. H., Qin, K., and Chan, P.: Unraveling Urban Nighttime Aerosol Characteristics and Meteorological Factors on AOD-PM Relationships in East Asia, Atmospheric Environment, 360, 121 388, https://doi.org/10.1016/j.atmosenv.2025.121388, 2025a.

https://doi.org/10.5194/egusphere-2026-1506
Preprint. Discussion started: 26 March 2026

Li, L., Li, M., Fan, X., Chen, Y., Lin, Z., Hou, A., Zhang, S., Zheng, R., and Chen, J.: Measurement Report: The Variation Properties of Aerosol Hygroscopic Growth Related to Chemical Composition during New Particle Formation Days in a Coastal City of Southeast China, Atmospheric Chemistry and Physics, 25, 3669–3685, https://doi.org/10.5194/acp-25-3669-2025, 2025b.

Li, Z., Li, K., Li, D., Yang, J., Xu, H., Goloub, P., and Victori, S.: Simple Transfer Calibration Method for a Cimel Sun–Moon Photometer: Calculating Lunar Calibration Coefficients from Sun Calibration Constants, Applied Optics, 55, 7624, https://doi.org/10.1364/AO.55.007624, 2016.

O'Neill, N. T., Ignatov, A., Holben, B. N., and Eck, T. F.: Citation for: The Lognormal Distribution as a Reference for Reporting Aerosol Optical Depth Statistics; Empirical Tests Using Multi-year, Multi-site AERONET Sunphotometer Data, AGU Journals, 2000.

O'Neill, N. T., Eck, T. F., Smirnov, A., Holben, B. N., and Thulasiraman, S.: Spectral Discrimination of Coarse and Fine Mode Optical Depth, Journal of Geophysical Research: Atmospheres, 108, https://doi.org/10.1029/2002JD002975, 2003.

Perrone, M. R., Lorusso, A., and Romano, S.: Diurnal and Nocturnal Aerosol Properties by AERONET Sun-Sky-Lunar Photometer Measurements along Four Years, Atmospheric Research, 265, 105 889, https://doi.org/10.1016/j.atmosres.2021.105889, 2022.

Román, R., González, R., Toledano, C., Barreto, Á., Pérez-Ramírez, D., Benavent-Oltra, J. A., Olmo, F. J., Cachorro, V. E., Alados-Arboledas, L., and De Frutos, Á. M.: Correction of a Lunar-Irradiance Model for Aerosol Optical Depth Retrieval and Comparison with a Star Photometer, Atmospheric Measurement Techniques, 13, 6293–6310, https://doi.org/10.5194/amt-13-6293-2020, 2020.

Sinyuk, A., Holben, B., Smirnov, A., Eck, T., Slutsker, I., Schafer, J., Giles, D., and Sorokin, M.: Assessment of Error in Aerosol Optical Depth Measured by AERONET Due to Aerosol Forward Scattering, Geophysical Research Letters, 39, 23 806, https://doi.org/10.1029/2012GL053894, 2012.

Song, J., Saathoff, H., Jiang, F., Gao, L., Zhang, H., and Leisner, T.: Sources of Organic Gases and Aerosol Particles and Their Roles in Nighttime Particle Growth at a Rural Forested Site in Southwest Germany, Atmospheric Chemistry and Physics, 24, 6699–6717, https://doi.org/10.5194/acp-24-6699-2024, 2024.

Stone, T. C., Kieffer, H., Lukashin, C., and Turpie, K.: The Moon as a Climate-Quality Radiometric Calibration Reference, Remote Sensing, 12, 1837, https://doi.org/10.3390/rs12111837, 2020.

Toledano, C., González, R., Fuertes, D., Cuevas, E., Eck, T. F., Kazadzis, S., Kouremeti, N., Gröbner, J., Goloub, P., Blarel, L., Román, R., Barreto, Á., Berjón, A., Holben, B. N., and Cachorro, V. E.: Assessment of Sun Photometer Langley Calibration at the High-Elevation Sites Mauna Loa and Izaña, Atmospheric Chemistry and Physics, 18, 14 555–14 567, https://doi.org/10.5194/acp-18-14555-2018, 2018.

Toledano, C., Taylor, S., Barreto, Á., Adriaensen, S., Berjón, A., Bialek, A., González, R., Woolliams, E., and Bouvet, M.: LIME: Lunar Irradiance Model of ESA, a New Tool for Absolute Radiometric Calibration Using the Moon, Atmospheric Chemistry and Physics, 24, 3649–3671, https://doi.org/10.5194/acp-24-3649-2024, 2024.

Wainwright, C., Chang, R. Y.-W., and Richter, D.: Aerosol Activation in Radiation Fog at the Atmospheric Radiation Program Southern Great Plains Site, AGU Journals, 2021.

Zhu J., Y. Zheng, Z. Xia, Y. Wang, J. Bi, K. Gui, L. Li, S. Liu, H. Zhang, H. Zhao, S. Peng, M. Ju, Y. Liang, H. Che, and X. Zhang: Retrieving Nocturnal Aerosol Optical Depth Using Lunar Photometry: Algorithm Improvements and Evaluation, IEEE Transactions on Geoscience and Remote Sensing, 64, 1–18, https://doi.org/10.1109/TGRS.2025.3642839, 2026.